# Role for DNA exonuclease V resection activity of RecBCD in control of aberrant chromosomal replication initiation in *Escherichia coli*

Sayantan Goswami[1,2,3] and J Gowrishankar[1,3]*

[1]Centre for DNA Fingerprinting and Diagnostics, Hyderabad 500039, India.

[2]Graduate Studies, Manipal Academy of Higher Education, Manipal 576104, India.

[3]Indian Institute of Science Education and Research Mohali, SAS Nagar 140306, India.

* To whom correspondence should be addressed: Prof J Gowrishankar (Orcid ID: 0000-0003-2483-9209), Tel: +91-172-2240266; Fax: +91-172-2240124; Email: shankar@iisermohali.ac.in

**Abstract**

Replication of the circular bacterial chromosome is initiated from a locus *oriC* with the aid of an essential protein DnaA. One approach to identify factors acting to prevent aberrant *oriC*-independent replication initiation has been that to obtain mutants which survive loss of DnaA. Here we show that a Δ*recD* mutation, associated with loss of RecBCD's double strand-DNA exonuclease V activity, provokes abnormal replication and rescues Δ*dnaA* lethality in two situations: (i) in absence of 5'-3' single-strand DNA exonuclease RecJ, or (ii) when multiple two-ended DNA double strand breaks (DSBs) are generated either by I-SceI endonucleolytic cleavages or by radiomimetic agents phleomycin or bleomycin. With two-ended DSBs in a Δ*recD* strain, Δ*dnaA* viability was retained even after linearization of the chromosome. Data from genome-wide DNA copy number determinations in Δ*dnaA*-rescued cells lead us to propose a model that exonuclease V-mediated DNA resection activity is critical for prevention of a σ-mode of rolling-circle over-replication when convergent replication forks merge and fuse; such mergers occur during normal replication at the chromosomal terminus region, as well as during repair of two-ended DSBs following "ends-in" replication. Resection mechanisms may also be important in eukaryotes to prevent DNA over-replication at sites of fork merger.

## Introduction

A requirement for timely and faithful duplication of a cell's genetic material is an essential feature of all life forms (1). The genome of most eubacteria, of which *Escherichia coli* is the prototype, is comprised of a single circular chromosome. Chromosomal replication is initiated (with the aid of an unstable yet essential initiator protein DnaA) at a specific locus *oriC* and proceeds bidirectionally across the pair of "replichores" for the forks to then meet and merge within a broad terminus region that is situated diametrically opposite *oriC* [reviewed in (2, 3)]. The terminus region is flanked at its ends by *Ter* sequences which represent binding sites for the Tus protein; the Tus-bound *Ter* sites act in a polar fashion to block progression of a replisome that has already traversed the terminus region from entering the opposite replichore, thus serving to limit most if not all fork mergers to occur within this region [reviewed in (2, 4, 5)]. Additional *Ter* sequences are also present on either replichore in the *oriC*-distal half of the chromosome, each so oriented as to block replisome progression towards *oriC* (2, 4, 5).

Replisomes often encounter impediments to their progression (in the form of lesions in, or protein complexes bound to, DNA) which may lead to their pausing, collapse or disintegration, and thereby to generation of a single broken DNA end or "one-ended" double strand break (DSB) (6–8). Mechanisms of repair by homologous recombination and of replication restart then operate at each of these sites to reconstitute a fresh replisome that resumes its directional progression towards the terminus [reviewed in (8, 9)]. Recombinational repair is comprised of the steps of DNA resection mediated by the RecBCD complex (which possesses DNA helicase and exonuclease V activities), followed by RecA-mediated annealing of a single-strand (ss) DNA 3' end into a homologous DNA duplex to generate a D-loop [reviewed in (9–15)]. Replication restart occurs from the D-loop and is mediated by the PriABC and DnaT proteins through one or more redundant pathways (6, 16). Incidentally, the same mechanisms of recombinational repair and replication restart are presumed also to operate at sites of two-ended DSBs to mediate "ends-in" replication and thus to restore circularity of the chromosome (6, 11, 13, 16); generation of such two-ended DSBs is replication-unrelated, and occurs upon

the action of endonucleases such as I-SceI or upon exposure to ionizing radiation or radiomimetic agents (17, 18) like phleomycin (Phleo) or bleomycin (Bleo).

The organization and replication of the chromosome of *E. coli* is characterized by several additional (and probably inter-dependent) features of interest, all of which are correlated with the *ori*-to-*Ter* directionality of its two replichores. First, the majority of heavily transcribed genes (including all seven ribosomal RNA [*rrn*] operons) are codirectional with replisome progression (2), and there is evidence that head-on transcription-replication conflicts engendered either by inversion of *rrn* operons (19) or by ectopic placement of *oriC* (20) is detrimental. Second, the chromosome is divided into a number of macrodomains that are symmetrically distributed across the two replichores (21, 22), although the details of such organization and their contribution to bacterial fitness are still under investigation. Third, the mechanisms of decatenation and segregation of sister chromatids, as well as those of cell division, have evolved to be coupled to replication of the chromosome terminus region (3).

A fourth feature of interest is the bias in distribution of two sets of *cis* sequences (Chi and KOPS) across the genome, that are both involved in functions related to the resolution of problems arising from collapsed or disintegrated replication forks (15, 23). The distributional bias of Chi serves to limit the extent of RecBCD-mediated DNA resection at one-ended DSB sites (10, 15), whereas that of KOPS is intended to facilitate monomerization of chromosome dimers that may be generated following recombinational repair (23).

Finally, *ori*-to-*Ter* directionality of replisome progression also imposes a defined gene dosage gradient across the two replichores in asynchronously growing populations of cells (2). The steepness of this gradient is accentuated in rapidly growing cultures because of the phenomenon of "multi-fork replication", wherein new rounds of replication are initiated at *oriC* even as the earlier pairs of forks have not reached the terminus region. Accordingly, highly expressed genes have also been favoured in evolution to be located closer to *oriC* than to the terminus.

Given that all of the features above require that chromosomal replication be initiated from the singular *oriC* locus, it is not surprising that mechanisms also exist in *E. coli* cells for avoidance of aberrant *oriC*-independent chromosomal replication. Such *oriC*-independent replication is also called stable DNA replication (SDR) since it persists even after transcription or translation have been inhibited in the cells (24).

One approach to delineate the mechanisms for avoidance of aberrant replication has been that to obtain mutants which retain viability in absence of DnaA (whose action is obligatory for replication initiation from *oriC*). Such mutants are said to exhibit constitutive SDR [cSDR (24)]. The mutations that have been so identified include those abrogating the functions of RNase HI (24–26); RecG helicase (25, 27); topoisomerase I (28); Dam DNA methylase (29); or different combinations of three redundant 3' ss-DNA exonucleases I, VII, and SbcCD, and a 5' ss-DNA exonuclease RecJ (30). In all of these cases, two additional mutations (Δ*tus* and *rpoB*35*) are also required for (or, in case of RNase HI deficiency, facilitate) DnaA-independent viability (25, 27–30); the two mutations presumably aid in the progression of *oriC*-independent replication completely around the circular chromosome, the former by disrupting the polar replication barriers at *Ter* sequences (4, 5) and the latter by resolving head-on collisions of transcription complexes with the replisome (31–34).

To further explore the mechanisms for avoidance of cSDR, we have in the present study studied additional conditions that serve to confer Δ*dnaA* viability in *E. coli*. Our results suggest that DNA exonuclease V resection activity of RecBCD [which is lost in Δ*recD* mutants (9, 10)] is critically required to prevent a rolling-circle type (that is, σ-mode) of over-replication from sites where convergent replication forks merge and fuse, and that the *rrn* operons represent a predominant source of transcription-replication conflict during *oriC*-independent replication.

## Materials and Methods

**Bacterial strains and plasmids**. Genotypes of *E. coli* strains are listed in Table S1. Knockout ($Kan^R$ insertion-deletion) alleles sourced from the Keio

collection (35) included the following: *dinG*, *rdgB*, *recA*, *recD*, *recG*, *recJ*, *sbcC*, *tus*, *xseA*, and *xonA*. The construction by recombineering of strains with distributed I-SceI sites on the chromosome is described in the *Supplementary Text*.

Previously described plasmids include: pKD13, pKD46, pKD78, and pCP20, for use in recombineering experiments and for Flp-mediated site-specific excision of FRT-flanked DNA segments (36); ASKA vector pCA24N and its derivatives expressing *recD*$^+$ or *recJ*$^+$ (37); ptRNA67 carrying six tRNA genes (38); and shelter plasmids pHYD2388 and pHYD4805 carrying *dnaA*$^+$ (29). Plasmid pHYD5301 was constructed in this study, as described in the *Supplementary Text*.

**Culture media and conditions.** Strains were routinely cultured in LB medium at 37° (39), and supplementation of growth media with Xgal or antibiotics ampicillin (Amp), chloramphenicol (Cm), kanamycin (Kan), spectinomycin (Sp), tetracycline (Tet), and trimethoprim (Tp) were at the concentrations described earlier (40). Phleo and Bleo were each added at 1 μg/ml, and L-arabinose (Ara) at 0.2%.

**Blue-white assay for determining viability of Δ*dnaA* derivatives.** The 'blue-white screening' strategy used to identify conditions that render a Δ*dnaA* mutant viable was as earlier described (28, 29). The parental strain is Δ*dnaA* (and Δ*lacZ*) on the chromosome and carries a single-copy-number Tp$^R$ *dnaA*$^+$ *lacZ*$^+$ shelter plasmid pHYD2388 whose equi-partitioning to daughter cells during cell division is inefficient; thus, typically around 5 to 20% of cells in a culture (grown in absence of Tp) are plasmid-free. The latter cells would be able to form colonies (white on Xgal-supplemented medium) only if cSDR in them was sufficient to confer viability. [Since plasmid loss frequency in this assay is relatively low, occurrence of white-sectored blue colonies is not as common as that in an analogous system described by other groups (32, 41) in which the proportion of plasmid-free cells was around 50%.] The parental strain also harbored Δ*tus* and *rpoB*35* mutations, which are expected to enable replication initiated from sites other than *oriC* to progress completely around the chromosome (27).

**Genome-wide DNA copy number determinations.** Copy number

determinations of different genomic regions were performed by whole-genome sequencing (WGS) on phenol-chloroform extracted DNA preparations, essentially as described (29, 42). WGS read data of 200-fold or greater coverage were generated with a paired-end sequencing strategy on an Illumina HiSeq platform. After alignment to the MG1655 reference genome (NC_000913.3), base read counts were determined for successive non-overlapping 1 kb intervals and were first normalized to the per-kb average of either (i) the aggregate of aligned base read counts, in the case of cultures not subjected to I-SceI cleavage, or (ii) read counts of the 500-kb region between genomic coordinates 683 kb and 1183 kb, for cultures subjected to I-SceI cleavage (since the latter region was expected to be the least affected by DNA resection following such cleavage in the different strains). A second normalization for all cultures was then done against interval-specific normalized read counts of the wild-type strain grown to stationary phase (data for which are shown in Fig. S4A). The moving average method for data smoothening was as described (29).

**Other methods.** The methods for phage P1 transduction (43); recombineering and Flp-recombinase-mediated site-specific excision between FRT sites (36); flow cytometry for cSDR detection (44, 45); and chromosome linearization with the aid of N15 phage and engineered *tos* sites (25, 27, 46) were as described. Protocols of Sambrook and Russell (47) were followed for recombinant DNA manipulations, PCR, and transformation.

## Results

**Approaches used to investigate cSDR.** Three approaches were used in this work to study occurrence and features of cSDR in different strains.

(i) As described above, a shelter plasmid-based 'blue-white screening' strategy was used initially to identify conditions that serve to rescue Δ*dnaA* lethality (28, 29).

(ii) In a second approach based on flow cytometry, the extent of continued DNA synthesis following addition of a protein synthesis inhibitor spectinomycin was investigated (29, 45). Since DnaA is unstable and needs to be synthesized afresh for each round of replication initiation at *oriC*, this

method provides a quantitation of cSDR occurring in individual cells.

(iii) Finally, a WGS approach was used to determine relative copy numbers of different chromosomal regions at the population level in cultures under cSDR conditions. Gradients of copy number distribution permit inferences of likely aberrant replication initiation sites (25–27, 29, 30, 44, 48). The WGS approach also serves as a quality check on strain genotypes and possible existence of suppressor mutations.

**Rescue of Δ*dnaA* lethality in a Δ*recD* mutant by imposition of two or more site-specific two-ended DSBs.** DNA damage also results in a type of SDR that is called inducible SDR [iSDR (24)]. We asked whether iSDR could be co-opted to rescue Δ*dnaA* lethality in particular situations; towards this end, we tested the combined effects of a Δ*recD* mutation and perturbations conferring iSDR.

The Δ*recD* mutation was chosen as candidate for the following reasons. Leach and coworkers had shown excessive DNA synthesis in the vicinity of a site-specific chromosomal DSB in a Δ*recD* mutant (49). Furthermore, copy number determinations by WGS in Δ*recD* strains (48, 49) have revealed a characteristic "mid-terminus peak" that is most commonly associated with mutants exhibiting cSDR (2, 26–30).

Viability in absence of DnaA was assessed by blue-white screening assays in strains (in a Δ*tus rpoB*35* background) in which iSDR was provoked after engineering up to four distributed I-SceI cleavage sites in the genome (locations of I-SceI sites used in this study are schematically depicted and numbered with Roman numerals in Fig. 1A). The derivatives also carried a chromosomal construct for Ara-induced expression of I-SceI enzyme (50). Previous studies have shown that <10% of wild-type cells that have suffered three discrete I-SceI cleavages on the chromosome retain their viability (51), which was also confirmed in our work (see Fig. 1C).

The results from these experiments, performed on Ara-supplemented media, indicate that Δ*dnaA* lethality is not rescued (i) even by four sites of I-SceI cleavage in a *recD*$^+$ strain (Fig. 1B ii-v), nor (ii) by a Δ*recD* mutation by itself or in combination with a single site of I-SceI cleavage (Fig. 1B vi-vii, respectively). On the other hand, rescue of Δ*dnaA* lethality did occur in Δ*recD*

mutants bearing two, three, or four I-SceI cleavage sites (Fig. 1B viii-x). Sustained viability of these Δ*dnaA* derivatives (white colonies) upon sub-culturing was contingent on supplementation of the growth medium with Ara (Fig. 1D), although the proportion of viable cells in strains with three or four cleavage sites was low; a viable Δ*dnaA rnhA* (RNase HI-deficient) derivative (see Fig. 8 iii for a representative blue-white panel) was used as control on these plates (Fig. 1D, top row).

**Two-ended DSBs generated by radiomimetic agents also rescue Δ*dnaA* lethality in Δ*recD* mutant.** Radiomimetic agents such as Phleo and Bleo mediate scission of both DNA strands to generate two-ended DSBs (17, 18).When these agents were tested at sublethal doses in the blue-white screening assay (in *recD*$^+$ or Δ*recD* strains that were Δ*tus rpoB*35*), Δ*dnaA* viability (that is, recovery of white colonies) was noted only with the combination of a Δ*recD* mutation and supplementation with Phleo or Bleo (Fig. 2A, compare v-vi with i-iv). Rescue of Δ*recD* Δ*dnaA* lethality on Phleo-supplemented medium was lost upon introduction of *recD*$^+$ on a plasmid, but not of the plasmid vector (Fig. 2B). Rescue was also dependent on presence of both Δ*tus* and *rpoB*35* mutations in the strain (Fig. S1A). Furthermore, as expected, the Δ*recD* white colonies obtained on Phleo-supplemented medium retained viability only on medium supplemented with sublethal Phleo (Fig. 2C, bottom row; Δ*dnaA rnhA* colony was used as control, top row).

Accordingly, we conclude that a discrete number of two-ended DSBs, generated by either radiomimetic agents or site-specific endonucleolytic cleavages, are necessary and sufficient to rescue Δ*dnaA* lethality in a Δ*recD* mutant.

**Perturbations that generate one-ended DSBs do not rescue Δ*dnaA* lethality in Δ*recD* strain.** Perturbations that generate nicks or abasic sites in DNA lead subsequently to collapse or disintegration of replication forks and thereby to one-ended DSBs on the chromosome. Such perturbations include mutations in genes *rdgB, polA,* or *dut* (9, 52, 53), or exposure to genotoxic agents such as norfloxacin, ciprofloxacin, 2-aminopurine, or mitomycin C (7, 9, 54). One- and two-ended DSBs are similar to one another in that (i) both provoke iSDR, and (ii) their repair is RecA- and RecBCD-dependent.

When one-ended DSB-generating perturbations were tested in a Δ*recD* mutant (carrying Δ*tus* and *rpoB*35* alleles), none was able to confer Δ*dnaA* lethality rescue (Fig. 3). These results therefore indicate that one- and two-ended DSBs behave dissimilarly in this assay with Δ*recD* strains.

**Rescue of Δ*dnaA* lethality by a combination of Δ*recD* and Δ*recJ* mutations.** We then asked whether any other single gene mutation, which by itself cannot rescue Δ*dnaA* lethality, can do so in combination with Δ*recD*. Of a variety of candidate genes tested, a Δ*recJ* mutation was shown to synergize with Δ*recD* to confer viability to a Δ*dnaA* mutant (Fig. 4A, compare iii with i-ii; see also Fig. 1D, row 2); the phenotype was complementable by plasmids expressing RecD or RecJ, but not by the empty vector (Fig. 4B, compare ii-iii with i). On the other hand, the combination of Δ*recD* with loss of any one of the other ss-DNA exonucleases ExoI, ExoVII, or SbcCD (encoded by *xonA*, *xseA* and *sbcCD*, respectively) could not rescue Δ*dnaA* lethality (Fig. S1B).

Loss of RecA was not lethal for the Δ*recD* Δ*recJ* strain (Fig. 4 iv, note presence of blue colonies), suggesting that spontaneous DSBs are not the cause of cSDR in the double mutant. On the other hand, rescue of Δ*dnaA* lethality was not observed in the triple mutant Δ*recD* Δ*recJ* Δ*recA* (Fig. 4 iv, note absence of white colonies).

Suppression of Δ*dnaA* inviability, both in the Δ*recD* Δ*recJ* strain and in Δ*recD* with Phleo, was abolished upon introduction of a *priA300* mutation (Fig. S2, i-ii); the latter is associated with loss of helicase activity of the replication restart protein PriA (6, 16). Another candidate mutation that was tested Δ*dinG* also abolished viability of Δ*dnaA* both in the Δ*recD* Δ*recJ* strain and in Δ*recD* on Phleo-supplemented medium (Fig. S2, iii-iv). The DinG helicase is required to facilitate progression of replisomes when they are in head-on conflict with *rrn* operon transcription (such conflicts are expected in cSDR), presumably by catalyzing removal of RNA-DNA hybrids generated at the sites of conflict (19); we could show that RNase HI overexpression (achieved from an ectopic chromosomal $P_{ara}$-*rnhA* construct) restores Δ*dnaA* rescue in the Δ*dinG* derivatives above (Fig. S2, vii-viii), whereas the control construct lacking *rnhA* was unable to do so (Fig. S2, v-vi).

**Demonstration by flow cytometry of cSDR in Δ*recD* derivatives.** In the

flow cytometric method for cSDR detection, incorporation of the nucleotide analog EdU (as detected with Alexa Fluor 488 staining) is used as a measure of DNA synthesis in individual cells after protein synthesis is inhibited by addition of spectinomycin (29, 45). The experiments were performed in Δ*tus rpoB*35* derivatives of different strains; we did not, however, employ the method for cultures that had been subjected to overt DNA damage (such as with Phleo or Bleo exposure, or I-SceI cleavage), since iSDR that is known to be provoked by such damage is biochemically indistinguishable from cSDR (24).

EdU incorporation in absence of spectinomycin was uniformly high for all strains tested (Fig. S3). Following spectinomycin treatment, the proportion of cells exhibiting DNA synthesis above threshold was (in percent): wild-type (negative control), 6; *rnhA* (positive control), 88; Δ*recJ*, 29; Δ*recD*, 36; Δ*recD* Δ*recJ*, 85; and Δ*recD* Δ*recJ* Δ*recA*, 25 (Fig. 5 i-vi, respectively). Of these, as described above, it is only the Δ*recD* Δ*recJ* derivative that is viable in absence of DnaA, and its EdU positivity was comparable to that in the positive control.

For the Δ*recD* Δ*recJ* mutant, we also determined the proportion of EdU-positive cells after spectinomycin treatment of the *tus*$^+$ *rpoB*$^+$ derivative, in order to assess the quantitative contribution to cSDR of the mutations in these genes (Fig. 5 vii). At 45%, this proportion was approximately one-half of that in the isogenic Δ*tus rpoB*35* strain.

Taken together, these data indicate that (i) substantial cSDR occurs even in a Δ*recD* mutant without overt DNA damage; (ii) in a Δ*recD* Δ*recJ* mutant, loss of RecA is associated with reduction of biochemical cSDR; and (iii) presence of Δ*tus* and *rpoB*35* mutations is correlated with increased EdU incorporation in cells inhibited for protein synthesis. The last observation serves to re-affirm the proposal (27) that replication initiated from sites other than *oriC* is impeded for its progression around the chromosome by Tus-bound *Ter* sites and by conflicts between transcription and replication. Our data also support the notion advanced earlier (24) that the genetic assay imposes a far more stringent threshold for detection of cSDR than do the biochemical assays.

**Genome-wide DNA copy number determinations in Δ*recD* derivatives**

**with Phleo supplementation or with Δ*recJ* mutation.** As mentioned above, replication initiation from *oriC* in asynchronously growing cultures is characterized by a bidirectional *oriC*-to-*Ter* gradient of copy number distributions, with this pattern being disturbed in mutants exhibiting cSDR (2). We performed WGS experiments in different Δ*recD* or Δ*recD* Δ*recJ* derivatives to determine, at the population level, the nature of such alterations and thus to obtain insights into cSDR mechanisms operating in them.

Given that rescue of Δ*dnaA* lethality, as a manifestation of cSDR, had been observed in this study for the Δ*recD* mutant with Phleo and for the double mutant Δ*recD* Δ*recJ*, the WGS experiments were performed for both these situations, using the *dnaA*$^+$ *tus*$^+$ *rpoB*$^+$ derivatives; the control cultures were the wild-type strain as well as its single mutant Δ*recJ* and Δ*recD* derivatives (all *dnaA*$^+$ *tus*$^+$ *rpoB*$^+$, without Phleo). Copy number distribution by WGS were also determined for the cultures that were viable in absence of DnaA (that is, Δ*dnaA* Δ*tus rpoB*35* Δ*recD* with Phleo, and Δ*dnaA* Δ*tus rpoB*35* Δ*recD* Δ*recJ*) as well as for their cognate *dnaA*$^+$ derivatives.

The cultures for wild-type as well as its Δ*recD* and Δ*recJ* single mutant derivatives exhibited the expected bidirectional *oriC*-to-*Ter* gradient in their DNA copy number distributions (Fig. 6 i-ii, and Fig. S4B, respectively). As mentioned above, a characteristic copy number feature associated with a variety of perturbations conferring cSDR is presence of a "mid-terminus peak", that is, an increased copy number of DNA of the terminus region in *dnaA*$^+$ *tus*$^+$ *rpoB*$^+$ derivatives (25–30, 44, 48). We have previously suggested that the mid-terminus peak represents a population averaging of copy number contributions from superimposed aberrantly initiated replication forks that have then been trapped between the Tus-bound *Ter* sites of the terminus (2). We note that this feature was preserved also for the two sets of perturbations (Δ*recD* with Phleo, and Δ*recD* Δ*recJ*) that were correlated with cSDR in the present study (Fig. 6 iii-iv, respectively). The peak was not observed in the isogenic Δ*tus rpoB*35* derivatives (Fig. 6 v-vi, respectively), which is consistent with the proposal (26, 27) that it arises because of fork-trapping at *Ter* sites to which Tus is bound; the copy number gradient in these derivatives was also flattened which, as discussed below, supports the notion

that cSDR in these cells is sufficiently robust to counteract the *oriC*-directed copy number gradient averaged from the population.

For the pair of Δ*dnaA* cultures (which were also Δ*tus rpoB*35*), absence of an *oriC* peak was as expected; the copy number distribution was more or less flat across the genome in the Δ*recD* derivative cultured with sublethal Phleo (Fig. 6 vii), whereas that in the Δ*recD* Δ*recJ* mutant exhibited a broad peak in the vicinity of the terminus region (Fig. 6 viii). In the Discussion below, these patterns are interpreted in the context of different sites of postulated aberrant replication initiation in the cultures.

**Genome-wide DNA copy number determinations in Δ*recD* derivatives with site-specific two-ended DSBs.** Since we had identified that Δ*dnaA* lethality can be rescued in a Δ*recD* strain also by imposition of two-ended DSBs at two or more discrete sites through I-SceI cleavage (in presence of Δ*tus* and *rpoB*35* mutations), we determined by WGS the DNA copy number distributions in four of these Δ*dnaA*-suppressed derivatives: three bearing different combinations of dual I-SceI sites (of which site II near *dusA* was common and the second numbered site I, III, or V was near *yihQ*, *yaiZ*, and *nadB*, respectively), and one with three I-SceI sites (II, IV and V). All cultures were grown in continuous presence of Ara since this was a requirement for their viability.

As controls, *dnaA*$^+$ derivatives of the *recD*$^+$ and Δ*recD* strains each carrying two I-SceI cleavage sites (II and V) were used in the WGS experiments after growth in continuous presence of Ara (both were also Δ*tus* and *rpoB*35*). Previous studies have shown that sustained cleavage in the wild-type strain at a single chromosomal I-SceI site results in attainment of an equilibrium between DNA resection on the one hand and DNA repair on the other, such that an asymmetric V-shaped pattern of reduction in DNA copy number is generated around the cleavage site; this dip in copy number extends to approximately 100 kb towards *oriC* and 200 kb towards *Ter* (42, 55)

The results from these population-level DNA copy number determinations are shown in Figure 7. In the *dnaA*$^+$ *recD*$^+$ control strain (Fig. 7 i), copy number reductions were observed in the vicinity of both I-SceI cleavage sites II and V, but its magnitude was apparently less than that

described in the previous studies for a single site of cleavage (42, 55); it is possible that either cleavage by I-SceI, or resection by RecBCD, becomes rate-limiting with more than one I-SceI site on the chromosome. In the *dnaA*$^+$ Δ*recD* derivative (Fig. 7 ii), copy number reductions at the I-SceI sites (II and V) were less than those in the *recD*$^+$ control, which is similar to that also described earlier for single-site cleavage (55).

In the different Δ*dnaA* Δ*recD* cultures rendered viable by I-SceI cleavages, DNA copy number patterns were consistent with the idea that aberrant replication was being initiated in the vicinity of the cleavage sites. Thus, in a derivative with the dual cleavage sites II and V (Fig. 7 iii), two distinct copy number peaks were observed, whereas in that with sites II and III (Fig. 7 iv), a broad peak was located approximately midway between the two loci; and in a derivative with sites I and II (which are very close to one another, as also to *oriC*), the copy number gradient resembled that for *oriC*-initiated replication itself (Fig. 7 v). Finally, in a Δ*dnaA* strain with three I-SceI sites (II, IV, V) that were somewhat evenly separated on the chromosome, the copy number distribution was approximately flat across the genome (Fig. 7 vi). The interpretations from these data with respect to the mechanism of cSDR in absence of RecD are provided in the Discussion.

**Effect of chromosome linearization on rescue of Δ*dnaA* lethality in Δ*recD* mutants.** *E. coli* cells whose chromosome has been linearized in its terminus region by use of the phage N15-*tos* system retain viability without any obvious fitness deficit (46). In the context of cSDR, it has been suggested (based on studies with N15-*tos*) that when the source of aberrant replication initiation is itself in the terminus region (as has been postulated for *recG* or 3'-exonuclease mutants), viability in absence of DnaA function is exhibited only if the chromosome is circular (25, 27, 30); on the other hand, RNase HI deficiency confers viability even in linear chromosome derivatives lacking DnaA (25).

With the aid of the blue-white screening assay, the effect of chromosome linearization by N15-*tos* on rescue of Δ*dnaA* lethality in different derivatives was tested. Our results support earlier findings (25, 27) that Δ*dnaA* lethality rescue (in a Δ*tus rpoB**35* background) by Δ*rnhA* is retained but that by Δ*recG*

is abolished after chromosome linearization (Fig. 8, compare, respectively, iii with iv and v with vi); they also show that with the linear-chromosome constructs, Δ*recD* with Phleo, but not Δ*recD* Δ*recJ*, is able to confer Δ*dnaA* viability (Fig. 8, compare, respectively, vii with viii and ix with x).

**Dispensability of *rpoB*35* for cSDR-mediated Δ*dnaA* viability in Δ*rrn* strains.** In all situations where cSDR has been shown to confer viability in absence of DnaA function, the *rpoB*35* mutation (along with Δ*tus*) is either required for, or enhances the degree of, lethality rescue (25, 27–30). The model is that *oriC*-independent replication encounters substantial conflicts with transcription which thereby limit its ability to cover the entire chromosome (2), and that *rpoB*35* facilitates this process by mitigating the deleterious consequences of transcription-replication conflict (31–34).

The seven *rrn* operons are amongst the most heavily transcribed loci in *E. coli*, all of which are oriented to be co-directional with *oriC*-initiated replication (2). It is also established that strains bearing *rrn* operon inversions suffer substantial conflict between transcription and replication (19). We therefore employed a genetic approach to ask whether it is conflict at the *rrn* operons that necessitates a requirement of *rpoB*35* for cSDR to confer Δ*dnaA* viability.

For this purpose, we employed derivatives of strains constructed by the late Cathy Squires and coworkers (38, 56), with deletions of three, five, or six of the seven *rrn* operons, to ask whether cSDR-mediated rescue of Δ*dnaA* lethality could now be observed in Δ*tus rpoB*$^+$ strains (that is, in absence of *rpoB*35*). For each of the cSDR-generating situations *rnhA* [which, on LB medium, can suppress Δ*dnaA* lethality only if the derivative also carries the Δ*tus* and *rpoB*35* alleles (25, 29)], *dam,* Δ*recD* with Phleo, or Δ*recD* Δ*recJ,* Δ*dnaA* viability was exhibited even in an *rpoB*$^+$ background when either five or six *rrn* operons had been deleted (Fig. 9 ix-xvi), whereas the control Δ*dnaA* derivatives without *rrn* deletion were inviable (Fig. 9 i-iv); suppression by *rnhA* was observed even in a derivative with deletion of three *rrn* operons (Fig. 9 v).

Taken together, these data support an interpretation that the principal role of *rpoB*35* in promoting growth of Δ*dnaA* strains by mutations conferring cSDR is to mitigate transcription-replication conflict at the *rrn* loci, which is

supported by evidence also from other genetic studies (20, 57, 58).

## Discussion

The roles of the dual function RecBCD helicase-exonuclease for recombinational repair of one-ended and two-ended DSBs have been well characterized; the enzyme catalyzes resection of the DSB end and then mediates formation of a RecA nucleoprotein filament on ss-DNA (9–14). RecBCD's actions have also been implicated in the handling of reversed replication forks (59, 60) as well as in fidelity of chromosomal terminus region inheritance (61–64).

The RecBC complex, in absence of RecD, is largely devoid of exonuclease V resection activity but retains helicase activity and is proficient for DSB repair (9, 14). Thus, the phenotype of a Δ*recD* mutant may be expected to offer insights into the roles of exonuclease V in functions apart from that of DSB repair.

Previous studies have demonstrated that plasmid DNA is over-replicated in *recD* mutants (48, 65, 66). Chromosomal DNA over-replication in these mutants has also been recorded in two situations, namely in the chromosomal terminus region (48, 49) and in the vicinity of a DSB generated at an engineered palindromic sequence on the lagging strand template behind a replication fork (49). For the latter, a model to explain the phenomenon of DNA amplification in the Δ*recD* mutant has been proposed that invokes uncoordinated invasion of the two DSB ends into an intact sister chromosome (49). The present study demonstrates that DNA over-replication in cells deficient for exonuclease V can indeed be sufficient to confer viability in absence of *oriC*-dependent replication, as further discussed below.

**Suppression of Δ*dnaA* lethality in Δ*recD* mutants.** We have shown here that in strains carrying the Δ*tus* and *rpoB*35* mutations, Δ*dnaA* inviability is suppressed by a Δ*recD* mutation in two situations: (i) when two-ended DSBs are generated, either with sublethal Phleo or Bleo or by two or more site-specific endonucleolytic cleavages mediated by I-SceI; or (ii) in absence of another DNA exonuclease RecJ. The former suppression is exhibited in strains with a circular or a linear chromosome, whereas the latter occurs only in strains with a circular chromosome. One-ended DSBs in the Δ*recD* mutant

do not support Δ*dnaA* viability.

The model which we propose to explain these findings draws on those outlined earlier by the groups of Courcelle (48, 64, 67, 68) and of Rudolph (27, 30), and is schematically depicted in Figure 10. In wild-type *E. coli*, the common feature between chromosomal terminus region replication on the one hand and ends-in replication during two-ended DSB repair on the other is that of convergent replication forks which subsequently merge (Fig. 10A); such fork mergers are not a feature of one-ended DSB repair. We suggest that the converging replisomes may cross one another, as was postulated earlier by the Rudolph and Courcelle labs (30, 64) and has also been shown to occur in eukaryotic systems (69). We further propose that this ultimately results in a structure in which each extended leading strand has displaced the lagging strand of the opposite fork to create a 5' flap, as shown in Figure 10B.

Should this model be correct, the intermediate processing steps between the structures depicted in panels A and B of Figure 10 would remain to be determined, as too the roles if any of different DNA helicases (DnaB, RecG, PriA), DNA polymerases (I, III), and DNA topoisomerases (gyrase, topoisomerases III and -IV) in mediating these events. It has been suggested earlier that when replisomes cross one another at a site of fork convergence, 3' flaps are initially generated which can then be converted to 5' flaps by action of RecG helicase (27, 30).

According to our model, the 5' flap that is generated then serves as template for synthesis of Okazaki fragments, similar to that occurring during rolling circle replication of λ phage in the late phase of its lytic cycle (70, 71); this would require replication restart mechanisms mediated by PriA/B/C to aid in replisome assembly at the 3-way junction. What then ensues is progressive synthesis of a linear DNA duplex which is reasonably stable in absence of exonuclease V.

In our model as shown in Figure 10B, two linear DNA duplexes are capable of being generated from a single pair of convergent replication forks in the Δ*recD* mutant, which would explain the bidirectional gradient of DNA copy number from I-SceI cleavage sites that is observed in the WGS studies. However, the possibility cannot be excluded that this bidirectionality is merely

a population phenomenon, and that it may not be a simultaneous occurrence in individual cells.

Our model would explain many of the observations from this and earlier studies. (i) Since the 5' flap is susceptible to RecJ-mediated degradation (which can happen prior to synthesis of the first Okazaki fragment), the extrusion process will be expected to be more efficient in a Δ*recD* Δ*recJ* mutant. Consequently, such synthesis from the chromosomal terminus region alone may be sufficient to support Δ*dnaA* viability in this mutant whereas in a Δ*recD* *recJ*$^+$ strain, additional converging fork pairs (at sites of two-ended DSB repair) would also be required for the purpose. (ii) As a corollary, since the locus of additional DNA synthesis is restricted to the terminus region of Δ*recD* Δ*recJ* mutants, it is rendered sensitive to chromosome linearization (25, 27, 30); on the other hand, since such synthesis is distributed across several sites in Δ*recD* mutants that have suffered two-ended DSBs, rescue of Δ*dnaA* lethality is observed even in the linear chromosome derivatives. (iii) The same features would also explain, respectively, the terminus region peak and flattened DNA copy number distribution patterns in cultures of Δ*dnaA* Δ*recD* Δ*recJ* and Δ*dnaA* Δ*recD* with Phleo. (iv) Many extruded DNA duplexes would undergo extension in the retrograde *Ter*-to-*oriC* direction, necessitating presence of the Δ*tus* and *rpoB***35* mutations to achieve replication of the entire chromosome in absence of DnaA. (v) Abolition of Δ*dnaA* rescue in Δ*recD* derivatives with *priA300* mutation can be correlated with compromise by the latter of replication restart (6, 16). Abolition by Δ*recA* can probably be explained by the fact that retrograde progression of the replisome (towards *oriC*) is likely to be impeded by frequent fork reversal events (60), whose resolution in strains deficient for exonuclease V is known to be RecA-dependent (41, 59). In our model, RecA will also be required for generation of intact circular chromosomes from the extruded linear DNA sequences by homologous recombination.

Leach and coworkers had used a strain in which SbcCD overexpression leads to cleavage of a palindrome on the lagging strand behind a replication fork to show that such cleavage leads in a Δ*recD* mutant to localized DNA amplification (49). In *recD*$^+$ strains, the palindrome cleavage is expected to

generate a one-ended DSB (since the *Ter*-proximal end would be resected back to the fork by exonuclease V), whereas in a Δ*recD* mutant the consequence will be a two-ended DSB (72). Our model for ends-in replication outcomes in a Δ*recD* mutant would therefore account for their observations.

In summary, therefore, our proposal is that RecBCD's exonuclease V DNA resection activity is critically important to control rolling-circle over-replication at merger sites of converging replication forks. Given that in eukaryotic cells replisome components have been shown to cross one another at sites of fork convergence (69), it is possible that DNA resection mechanisms are also important for proper replication termination in eukaryotes.

**Role of ss-DNA exonucleases.** Apart from RecJ which is a ss-DNA exonuclease with 5'-3' polarity, there are at least three partially redundant ss-DNA exonucleases Exo I, Exo VII, and SbcCD with 3'-5' polarity (30, 73–75); the quadruple mutant is cold-sensitive for growth and is $UV^S$ (75, 76). Rudolph, Lloyd, and coworkers have previously suggested a role for the 3' ss-DNA exonucleases during the merger process of convergent replication forks in the terminus region (27, 30), which may not be mutually exclusive with the model being proposed in this study. We found that of these different ss-DNA exonucleases, it is RecJ deficiency alone that can singly synergize with Δ*recD* to rescue Δ*dnaA* lethality. It is likely that redundancy explains the failure of other ss-DNA exonucleases to do so. Midgley-Smith et al (30) et al have recently shown that deficiency of different ss-DNA exonuclease combinations can also confer cSDR.

## Data availability

The genome sequence and flow cytometry data described in this work are available for full public access from the repositories at https://www.ncbi.nlm.nih.gov/bioproject/842492 and https://flowrepository.org/id/FR-FCM-Z5F3, respectively.

## Supplementary data

Supplementary data are provided in a PDF file "Supplementary data".

## Funding

This work was supported by Government of India funds from (i) DBT Centre of Excellence (COE) project for Microbial Biology – Phase 2, (ii) SERB project CRG/ 2018/ 000348, and (iii) DBT project BT/ PR34340/ BRB/ 10/ 1815/ 2019. SG was recipient of a CSIR Research fellowship, and JG was recipient of the J C Bose fellowship and INSA Senior Scientist award.

We declare that there are no conflicts of interest.

## Acknowledgements

We thank Olivier Espéli, Mohan Joshi, Susan Rosenberg, and the late Cathy Squires for strains; Nalini Raghunathan and Apuratha Pandiyan for assistance with flow cytometry and WGS data analysis; Manjula Reddy, Abhijit Sardesai, and R Harinarayanan for comments on the manuscript; Christian Rudolph and COE team members for advice and discussions.

## References

1. Ekundayo,B. and Bleichert,F. (2019) Origins of DNA replication. *PLoS Genet.*, **15(9)**: e1008320.

2. Gowrishankar,J. (2015) End of the beginning: elongation and termination features of alternative modes of chromosomal replication initiation in bacteria. *PLoS Genet.*, **11(1)**: e1004909.

3. Reyes-Lamothe,R., Nicolas,E. and Sherratt,D.J. (2012) Chromosome replication and segregation in bacteria. *Annu. Rev. Genet.*, **46**, 121–143.

4. Neylon,C., Kralicek,A.V., Hill,T.M. and Dixon,N.E. (2005) Replication termination in *Escherichia coli*: structure and antihelicase activity of the Tus-Ter complex. *Microbiol. Mol. Biol. Rev.*, **69(3)**, 501–526.

5. Duggin,I.G., Wake,R.G., Bell,S.D. and Hill,T.M. (2008) The replication fork trap and termination of chromosome replication. *Mol. Microbiol.*, **70(6)**, 1323–1333.

6. Michel,B., Sinha,A.K. and Leach,D.R.F. (2018) Replication fork breakage and restart in *Escherichia coli. Microbiol. Mol. Biol. Rev.*, **82(3)**: e00013-18.

7. Kuzminov,A. (1995) Collapse and repair of replication forks in *Escherichia coli. Mol. Microbiol.*, **16**, 373–384.

8. Cox,M.M., Goodman,M.F., Kreuzer,K.N., Sherratt,D.J., Sandler,S.J. and Marians,K.J. (2000) The importance of repairing stalled replication forks. *Nature*, **404**, 37-41

9. Kuzminov,A. (1999) Recombinational repair of DNA damage in *Escherichia coli* and bacteriophage λ. *Microbiol. Mol. Biol. Rev.*, **63(4)**, 751–813.

10. Kuzminov,A. (2011) Homologous recombination-experimental systems, analysis, and significance. *EcoSal Plus*, **4(2)**:10.1128/ecosalplus.7.2.6

11. Sinha,A.K., Possoz,C. and Leach,D.R.F. (2020) The roles of bacterial dna double-strand break repair proteins in chromosomal DNA replication. *FEMS Microbiol. Rev.*, **44(3)**, 351–368.

12. Đermić,D. (2015) Double-strand break repair mechanisms in *Escherichia coli*: recent insights. *Adv. Genomics Genet.*, **5**, 35–42.

13. Kowalczykowski,S.C. (2015) An overview of the molecular mechanisms of recombinational DNA repair. *Cold Spring Harb. Perspect. Biol.*, **7(11)**: a0164410.

14. Dillingham,M.S. and Kowalczykowski,S.C. (2008) RecBCD enzyme and the repair of double-stranded DNA breaks. *Microbiol. Mol. Biol. Rev.*, **72(4)**, 642–671.

15. Smith,G.R. (2012) How RecBCD enzyme and chi promote DNA break repair and recombination: a molecular biologist's view. *Microbiol. Mol. Biol. Rev.*, **76(2)**, 217–228.

16. Michel,B. and Sandler,S.J. (2017) Replication restart in bacteria. *J. Bacteriol*, **199(13)**: e00102-17.

17. Suzuki,H., Nagai,K., Akutsu,E., Yamaki,H., Tanaka,N. and Umezawa,H. (1970) On the mechanism of action of bleomycin: strand scission of DNA cause by bleomycin and its binding to DNA in vitro. *J. Antibiot.* , **23(10)**, 473–480.

18. Sleigh,M.J. (1976) The mechanism of DNA breakage by phleomycin in vitro. *Nucleic Acids Res.*, **3(4)**, 891–901.

19. Boubakri,H., de Septenville,A.L., Viguera,E. and Michel,B. (2010) The helicases DinG, Rep and UvrD cooperate to promote replication across transcription units in vivo. *EMBO J.*, **29**, 145–157.

20. Ivanova,D., Taylor,T., Smith,S.L., Dimude,J.U., Upton,A.L., Mehrjouy,M.M., Skovgaard,O., Sherratt,D.J., Retkute,R. and Rudolph,C.J. (2015) Shaping the landscape of the *Escherichia coli* chromosome: replication-transcription encounters in cells with an ectopic replication origin. *Nucleic Acids Res.*, **43(16)**, 7865–7877.

21. Boccard,F., Esnault,E. and Valens,M. (2005) Spatial arrangement and macrodomain organization of bacterial chromosomes. *Mol. Microbiol.*, **57(1)**, 9-16.

22. Esnault,E., Valens,M., Espéli,O. and Boccard,F. (2007) Chromosome structuring limits genome plasticity in *Escherichia coli*. *PLoS Genet.*, **3(12)**, e226.

23. Bigot,S., Saleh,O.A., Lesterlin,C., Pages,C., el Karoui,M., Dennis,C., Grigoriev,M., Allemand,J.F., Barre,F.X. and Cornet,F. (2005) KOPS: DNA motifs that control *E. coli* chromosome segregation by orienting the FtsK translocase. *EMBO J.*, **24**, 3770–3780.

24. Kogoma,T. (1997) Stable DNA replication: interplay between DNA replication, homologous recombination, and transcription. *Microbiol. Mol. Biol. Rev.*, **61(2)**, 212–238.

25. Dimude,J.U., Stockum,A., Midgley-Smith,S.L., Upton,A.L., Foster,H.A., Khan,A., Saunders,N.J., Retkute,R. and Rudolph,C.J. (2015) The consequences of replicating in the wrong orientation: bacterial chromosome duplication without an active replication origin. *mBio*, **6**: e01294-15

26. Maduike,N.Z., Tehranchi,A.K., Wang,J.D. and Kreuzer,K.N. (2014) Replication of the *Escherichia coli* chromosome in RNase HI-deficient cells: multiple initiation regions and fork dynamics. *Mol. Microbiol.*, **91**, 39–56.

27. Rudolph,C.J., Upton,A.L., Stockum,A., Nieduszynski,C.A. and Lloyd,R.G. (2013) Avoiding chromosome pathology when replication forks collide. *Nature*, **500(7464)**, 608–611.

28. Leela,J.K., Raghunathan,N. and Gowrishankar,J. (2021) Topoisomerase I essentiality, DnaA-independent chromosomal replication, and transcription-replication conflict in *Escherichia coli*. *J. Bacteriol*, **203**: e00195-21.

29. Raghunathan,N., Goswami,S., Leela,J.K., Pandiyan,A. and Gowrishankar,J. (2019) A new role for *Escherichia coli* Dam DNA methylase in prevention of aberrant chromosomal replication. *Nucleic Acids Res.*, **47(11)**, 5698–5711.

30. Midgley-Smith,S.L., Dimude,J.U. and Rudolph,C.J. (2019) A role for 3' exonucleases at the final stages of chromosome duplication in *Escherichia coli*. *Nucleic Acids Res.*, **47(4)**, 1847–1860.

31. McGlynn,P. and Lloyd,R.G. (2000) Modulation of RNA polymerase by (p)ppGpp reveals a RecG-dependent mechanism for replication fork progression. *Cell*, **101(1)**, 35–45.

32. Trautinger,B.W., Jaktaji,R.P., Rusakova,E. and Lloyd,R.G. (2005) RNA polymerase modulators and dna repair activities resolve conflicts between DNA replication and transcription. *Mol. Cell*, **19(2)**, 247–258.

33. Dutta,D., Shatalin,K., Epshtein,V., Gottesman,M.E. and Nudler,E. (2011) Linking RNA polymerase backtracking to genome instability in *E. coli*. *Cell*, **146(4)**, 533–543.

34. Kamarthapu,V., Epshtein,V., Benjamin,B., Proshkin,S., Mironov,A., Cashel,M. and Nudler,E. (2016) ppGpp couples transcription to DNA repair in *E. coli*. *Science*, **352(6288)**, 993–996.

35. Baba,T., Ara,T., Hasegawa,M., Takai,Y., Okumura,Y., Baba,M., Datsenko,K.A., Tomita,M., Wanner,B.L. and Mori,H. (2006) Construction of *Escherichia coli* K-12 in-frame, single-gene knockout mutants: the Keio collection. *Mol. Syst. Biol.*, **2**:2006.0008.

36. Datsenko,K.A. and Wanner,B.L. (2000) One-step inactivation of chromosomal genes in *Escherichia coli* K-12 using PCR products. *Proc. Natl. Acad. Sci. U. S. A.*, **97(12)**, 6640–6645.

37. Kitagawa,M., Ara,T., Arifuzzaman,M., Ioka-Nakamichi,T., Inamoto,E., Toyonaga,H. and Mori,H. (2005) Complete set of ORF clones of *Escherichia coli* ASKA library (a complete set of *E. coli* K-12 ORF archive): unique resources for biological research. *DNA Res.*, **12(5)**, 291–299.

38. Zaporojets,D., Frenc,S. and Squires,C.L. (2003) Products transcribed from rearranged *rrn* genes of *Escherichia coli* can assemble to form functional ribosomes. *J. Bacteriol*, **185(23)**, 6921–6927.

39. Miller J.H. (1992) A Short Course in Bacterial Genetics: A Laboratory Manual and Handbook for *Escherichia coli* and related bacteria. Cold Spring Harbor Lab Press, New York.

40. Anupama,K., Leela,J.K. and Gowrishankar,J. (2011) Two pathways for RNase E action in *Escherichia coli* in vivo and bypass of its essentiality in mutants defective for Rho-dependent transcription termination. *Mol. Microbiol.*, **82(6)**, 1330–1348.

41. Mahdi,A.A., Buckman,C., Harris,L. and Lloyd,R.G. (2006) Rep and PriA helicase activities prevent RecA from provoking unnecessary recombination during replication fork repair. *Genes Dev.*, **20(15)**, 2135–2147.

42. Mallikarjun,J. and Gowrishankar,J. (2022) Essential role for an isoform of *Escherichia coli* translation initiation factor IF2 in repair of two-ended DNA double-strand breaks. *J. Bacteriol*, **204(4)**: e0057121.

43. Gowrishankar,J. (1985) Identification of osmoresponsive genes in *Escherichia coli*: evidence for participation of potassium and proline transport systems in osmoregulation. *J. Bacteriol*, **164(1)**, 434–445.

44. Brochu,J., Vlachos-Breton,É., Sutherland,S., Martel,M. and Drolet,M. (2018) Topoisomerases I and III inhibit R-loop formation to prevent

unregulated replication in the chromosomal Ter region of *Escherichia coli*. *PLoS Genet.*, **14**: e1007668.

45. Martel,M., Balleydier,A., Sauriol,A. and Drolet,M. (2015) Constitutive stable DNA replication in *Escherichia coli* cells lacking type 1A topoisomerase activity. *DNA Repair (Amst).*, **35**, 37–47.

46. Cui,T., Moro-oka,N., Ohsumi,K., Kodama,K., Ohshima,T., Ogasawara,N., Mori,H., Wanner,B., Niki,H. and Horiuchi,T. (2007) *Escherichia coli* with a linear genome. *EMBO Rep.*, **8**, 181–187.

47. Sambrook J. and Russell D. (2001) Molecular Cloning: A Laboratory Manual 3rd ed. Cold Spring Harbor Lab Press, New York.

48. Wendel,B.M., Courcelle,C.T. and Courcelle,J. (2014) Completion of DNA replication in *Escherichia coli*. *Proc. Natl. Acad. Sci. U. S. A.*, **111(46)**, 16454–16459.

49. White,M.A., Azeroglu,B., Lopez-Vernaza,M.A., Hasan,A.M.M. and Leach,D.R.F. (2018) RecBCD coordinates repair of two ends at a DNA double-strand break, preventing aberrant chromosome amplification. *Nucleic Acids Res.*, **46(13)**, 6670–6682.

50. Ponder,R.G., Fonville,N.C. and Rosenberg,S.M. (2005) A switch from high-fidelity to error-prone DNA double-strand break repair underlies stress-induced mutation. *Mol. Cell*, **19(6)**, 791–804.

51. Meddows,T.R., Savory,A.P., Grove,J.I., Moore,T. and Lloyd,R.G. (2005) RecN protein and transcription factor DksA combine to promote faithful recombinational repair of DNA double-strand breaks. *Mol. Microbiol.*, **57(1)**, 97–110.

52. Bradshaw,J.S. and Kuzminov,A. (2003) RdgB acts to avoid chromosome fragmentation in *Escherichia coli*. *Mol. Microbiol.*, **48(6)**, 1711–1725.

53. Ting,H., Kouzminova,E.A. and Kuzminov,A. (2008) Synthetic lethality with the dut defect in *Escherichia coli* reveals layers of DNA damage of increasing complexity due to uracil incorporation. *J. Bacteriol*, **190(17)**, 5841–5854.

54. Pohlhaus,J.R. and Kreuzer,K.N. (2005) Norfloxacin-induced DNA gyrase cleavage complexes block *Escherichia coli* replication forks, causing double-stranded breaks in vivo. *Mol. Microbiol.*, **56**, 1416–1429.

55. Sivaramakrishnan,P., Sepúlveda,L.A., Halliday,J.A., Liu,J., Núñez,M.A.B., Golding,I., Rosenberg,S.M. and Herman,C. (2017) The transcription fidelity factor GreA impedes DNA break repair. *Nature*, **550(7675)**, 214–218.

56. Asai,T., Condon,C., Voulgaris,J., Zaporojets,D., Shen,B., Al-Omar,M., Squires,C. and Squires,C.L. (1999) Construction and initial

characterization of *Escherichia coli* strains with few or no intact chromosomal rRNA operons. *J. Bacteriol*, **181(12)**, 3803–3809.

57. Veetil,R.T., Malhotra,N., Dubey,A. and Seshasayee,A.S.N. (2020) Laboratory evolution experiments help identify a predominant region of constitutive stable DNA replication initiation. *mSphere*, **5(1)**: e00939-19.

58. Syeda,A.H., Dimude,J.U., Skovgaard,O. and Rudolph,C.J. (2020) Too much of a good thing: how ectopic DNA replication affects bacterial replication dynamics. *Front. Microbiol.*, **11**:534.

59. Seigneur,M., Bidnenko,V., Ehrlich,S.D. and Michel,B. (1998) RuvAB acts at arrested replication forks. *Cell*, **95(3)**, 419–430.

60. de Septenville,A.L., Duigou,S., Boubakri,H. and Michel,B. (2012) Replication fork reversal after replication-transcription collision. *PLoS Genet.*, **8(4)**: e1002622.

61. Sinha,A.K., Durand,A., Desfontaines,J.M., Iurchenko,I., Auger,H., Leach,D.R.F., Barre,F.X. and Michel,B. (2017) Division-induced DNA double strand breaks in the chromosome terminus region of *Escherichia coli* lacking RecBCD DNA repair enzyme. *PLoS Genet.*, **13(10)**: e1006895.

62. Sinha,A.K., Possoz,C., Durand,A., Desfontaines,J.M., Barre,F.X., Leach,D.R.F. and Michel,B. (2018) Broken replication forks trigger heritable DNA breaks in the terminus of a circular chromosome. *PLoS Genet.*, **14(3)**: e1007256.

63. Cockram,C.A., Filatenkova,M., Danos,V., el Karoui,M. and Leach,D.R.F. (2015) Quantitative genomic analysis of RecA protein binding during DNA double-strand break repair reveals RecBCD action in vivo. *Proc. Natl. Acad. Sci. U. S. A.*, **112(34)**: e4735–42.

64. Courcelle,J., Wendel,B.M., Livingstone,D.D. and Courcelle,C.T. (2015) RecBCD is required to complete chromosomal replication: implications for double-strand break frequencies and repair mechanisms. *DNA Repair (Amst.)*, **32**, 86–95.

65. Cohen,A. and Clark,A.J. (1986) Synthesis of linear plasmid multimers in *Escherichia coli* K-12. *J. Bacteriol*, **167(1)**, 327–335.

66. Ogura,T., Hironori,N., Kano,Y., Imamoto,F. and Hiraga,S. (1990) Maintenance of plasmids in HU and IHF mutants of *Escherichia coli. Mol. Gen. Genet.*, **220(2)**, 197–203.

67. Wendel,B.M., Cole,J.M., Courcelle,C.T. and Courcelle,J. (2017) SbcC-SbcD and ExoI process convergent forks to complete chromosome replication. *Proc. Natl. Acad. Sci. U. S. A.*, **115(2)**, 349–354.

68. Hamilton,N.A., Wendel,B.M., Weber,E.A., Courcelle,C.T. and Courcelle,J. (2019) RecBCD, SbcCD and ExoI process a substrate created by

convergent replisomes to complete DNA replication. *Mol. Microbiol.*, **111(6)**, 1638–1651.

69. Dewar,J.M. and Walter,J.C. (2017) Mechanisms of DNA replication termination. *Nat. Rev. Mol. Cell Biol.*, **18(8)**, 507–516.

70. Takahashi,S. (1974) The rolling-circle replicative structure of a bacteriophage lambda DNA. *Biochem. Biophys. Res. Commun.*, **61(2)**, 657–663.

71. Baranska,S., Gabig,M., Wegrzyn,A., Konopa,G., Herman-Antosiewicz,A., Hernandez,P., Schvartzman,J.B., Helinski,D.R. and Wegrzyn,G. (2001) Regulation of the switch from early to late bacteriophage λ DNA replication. *Microbiology*, **147(Pt 3)**, 535–547.

72. Yasmin,T., Azeroglu,B., Cockram,C.A. and Leach,D.R.F. (2021) Distribution of Holliday junctions and repair forks during *Escherichia coli* DNA double-strand break repair. *PLoS Genet.*, **17(8)**: e1009717.

73. Viswanathan,M. and Lovett,S.T. (1998) Single-strand DNA-specific exonucleases in *Escherichia coli*: roles in repair and mutation avoidance. *Genetics*, **149(1)**, 7–16.

74. Đermić,D. (2006) Functions of multiple exonucleases are essential for cell viability, DNA repair and homologous recombination in *recD* mutants of *Escherichia coli*. *Genetics*, **172(4)**, 2057–2069.

75. Thoms,B., Borchers,I. and Wackernagel,W. (2008) Effects of single-strand DNases ExoI, RecJ, ExoVII, and SbcCD on homologous recombination of *recBCD*$^+$ strains of *Escherichia coli* and roles of SbcB15 and XonA2 ExoI mutant enzymes. *J. Bacteriol*, **190(1)**, 179–192.

76. Burdett,V., Baitinger,C., Viswanathan,M., Lovett,S.T. and Modrich,P. (2001) In vivo requirement for RecJ, ExoVII, ExoI, and ExoX in methyl-directed mismatch repair. *Proc. Natl. Acad. Sci. U. S. A.*, **98(12)**, 6765–6770.

## Legends to figures

**Figure 1:** Rescue of Δ*dnaA* lethality by I-SceI cleavages in Δ*recD* mutant. **(A)** Schematic depiction of locations on *E. coli* chromosome of different I-SceI sites used in the study (marked I to VI); also shown are positions of *oriC*, seven *rrn* operons, and terminus region flanked by *TerA* and *TerB/C*. **(B)** Blue-white assays for *recD*$^+$ and Δ*recD* derivatives each carrying the indicated number of I-SceI sites (positions denoted in parentheses); all strains (i) were Δ*dnaA* with *dnaA*$^+$ shelter plasmid pHYD2388, (ii) carried the gene encoding I-SceI enzyme under control of $P_{ara}$, and (iii) were plated on Ara-supplemented medium. Representative images are shown, and the numbers beneath each of the panels indicate the percentage of white colonies to the total, that is, viable even in absence of *dnaA*$^+$ shelter plasmid (minimum of 500 colonies counted). Examples of white colonies are marked by yellow arrows. Strains employed for the different sub-panels were pHYD2388 derivatives of (all strain numbers are prefixed with GJ): i, 16079; ii, 15853; iii, 15857; iv, 15861; v, 15864; vi, 16080; vii, 15888; viii, 15892; ix, 15896; and x, 15899. **(C, D)** Dilution-spotting assays on plates supplemented with 0.2% glucose (Glu) or Ara, of blue or white colonies sourced from plates of panel B; for the top two rows on the plates of panel D, the white colonies were sourced from plates shown, respectively, in Fig. 8 iii and Fig. 4 iii.

**Figure 2:** Rescue of Δ*dnaA* lethality by Δ*recD* in presence of sublethal Phleo or Bleo. **(A, B)** Blue-white assay results with pHYD2388 derivatives of GJ18607 (*recD*$^+$) or GJ15935 (Δ*recD*) are depicted as described in legend to Fig. 1B, on plates without or with Phleo or Bleo supplementation. In panel B, the Δ*recD* strain also carried the ASKA plasmid vector (pCA24N) or the latter's *recD*$^+$ derivative. **(C)** Dilution-spotting assays on medium without or with Phleo supplementation, of white colonies from plates shown in Fig. 8 iii (for top row) and Fig. 2A v (for bottom row).

**Figure 3:** Δ*dnaA* lethality is not rescued in Δ*recD* strain by perturbations generating one-ended DSBs. Blue-white assay results are depicted, as described in legend to Fig. 1B, for Δ*recD* derivatives subjected to one-ended DSBs through either additional mutations (panels i-iii) or exposure to

genotoxic agents (panels iv-vii), as indicated. Concentrations used were (µg/ml): norfloxacin, 0.02; ciprofloxacin, 0.005; mitomycin C, 1; and 2-aminopurine, 20. Strains used for the different panels were pHYD2388 derivatives of the following (all strain numbers are prefixed with GJ): i, 15939; ii, 15940; iii, 16082; and iv-vii, 15936.

**Figure 4:** Rescue of Δ*dnaA* lethality by Δ*recD* Δ*recJ*. **(A, B)** Blue-white assay results are depicted, as described in legend to Fig. 1B, for derivatives whose relevant genotypes are given on top (all were Δ*dnaA*/*dnaA*$^+$). Strains used for different sub-panels of panel A were pHYD2388 derivatives of the following (all strain numbers are prefixed with GJ): i, 15936; ii, 16083; iii, 15949; and iv, 16084. In panel B, the pHYD2388 derivative of Δ*recD* Δ*recJ* strain GJ15949 also carried the ASKA plasmid vector (pCA24N) or the latter's *recD*$^+$ or *recJ*$^+$ derivative.

**Figure 5**: Demonstration by flow cytometry of cSDR in Δ*recD* Δ*recJ* mutants. DNA synthesis was measured as described (29, 45), for different strains (genotype given on top of each panel) after addition of spectinomycin to the cultures. In each panel, the percentage of cells in which the fluorescence value exceeded the threshold (denoted by vertical line) set at 2 X $10^3$ arbitrary units (A.U.) is given at top right. Strains used for the different panels were (all strain numbers are prefixed with GJ): i, 18609; ii, 15981; iii, 15985; iv, 15984; v, 15986; vi, 15987; and vii, 15979.

**Figure 6**: Chromosomal DNA copy number analysis by WGS. Distinguishing strain genotypes and Phleo supplementation were as indicated on top of the panels. DNA copy numbers are plotted (after normalization) as moving averages across the genome. For these graphical representations, the circular 4642-kb long chromosome is shown linearized at *oriC*, with genome coordinates on the abscissa corresponding to the MG1655 reference sequence (wherein *oriC* is at 3926 kb); the positions of *TerA* and *TerC/B* are marked. Strains used for the different panels were (all strain numbers are prefixed with GJ): i, 18601, ii-iii, 15988; iv, 15991; v, 15984; vi, 15986; vii, 15936; and viii, 15949.

**Figure 7**: Chromosomal copy number distributions, as determined by WGS, in Δ*dnaA* Δ*recD* strains rendered viable by I-SceI cleavages. Distinguishing strain genotypes are indicated on top of the panels, and Roman numerals within parentheses denote the distinct I-SceI sites as shown in Fig. 1A; all strains also carried the construct for Ara-inducible expression of I-SceI enzyme, and were cultured in continuous presence of Ara for these experiments. Representations of WGS analysis data and notations used are as in the legend to Fig. 6; positions of I-SceI sites are also marked in each of the panels. Strains used for the different panels were (all strain numbers are prefixed with GJ): i, 15857/pHYD2388; ii, 15892/pHYD2388; iii, 15892; iv, 15889; v, 15890; and vi, 15896.

**Figure 8**: Effect of chromosome linearization on rescue of Δ*dnaA* lethality by different perturbations. Blue-white assay results are depicted, as described in legend to Fig. 1B, for isogenic pairs of circular- and linear-chromosome strains (upper and lower rows, respectively) with relevant perturbations as indicated on top. The proportion of white colonies to total was consistently elevated in *rnhA* mutants compared to that in other strains (see also Fig. 9), the reasons for which remain to be determined. Strains used for the different panels were pHYD2388 derivatives of the following (all strain numbers are prefixed with GJ): i, 18607; ii, 15993; iii, 16081; iv, 15995; v, 16464; vi, 15999; vii, 15936; viii, 16001; ix, 15949; and x, 16003.

**Figure 9**: Dispensability of *rpoB*35* for cSDR-mediated Δ*dnaA* viability in Δ*rrn* strains. Blue-white assay results are depicted, as described in legend to Fig. 1B, for strains whose genotypes are indicated on top of the panels, and which bear the indicated number of *rrn* operon deletions as indicated on left for each row. Strains used for the different panels were pHYD2388 derivatives of the following (in order from left to right for each row; all strain numbers are prefixed with GJ): Nil, 16074 to 16077; Δ3, 16033 to 16036; Δ5, 16053 to 16056; and Δ6, 16063 to 16066.

**Figure 10**: Model to explain cSDR in strains lacking RecD and RecJ. (**A**) Schematic depiction of disposition of DNA strands at a site of converging

replication forks, as would occur (i) in the chromosomal terminus region before replication termination, and (ii) during ends-in replication for two-ended DSB repair. (**B**) Progression of components of one replisome past those of the other is postulated to result, ultimately, in generation of a 5'-flap (red) on the opposite lagging strand and assembly of replication restart machinery to initiate a type of rolling-circle (σ-mode) replication. Please see text for details.

**Figure 1**

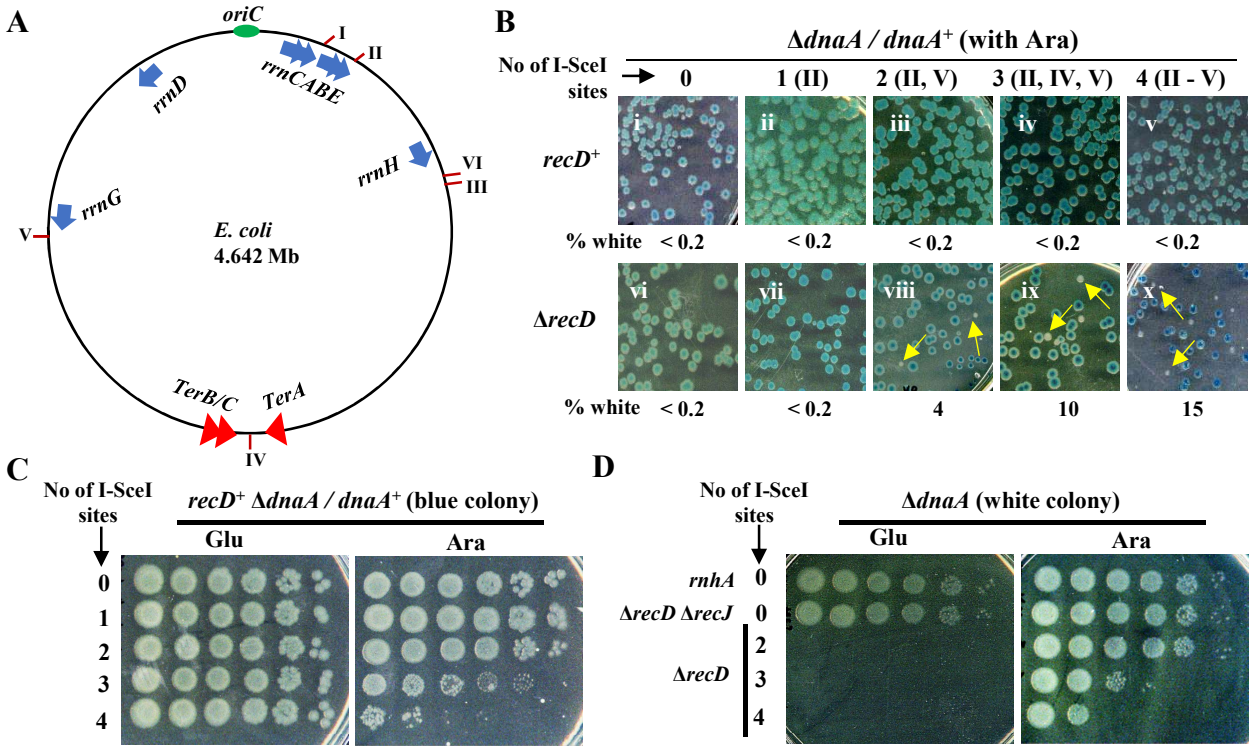


**Figure 1:** Rescue of Δ*dnaA* lethality by I-SceI cleavages in Δ*recD* mutant. **(A)** Schematic depiction of locations on *E. coli* chromosome of different I-SceI sites used in the study (marked I to VI); also shown are positions of *oriC*, seven *rrn* operons, and terminus region flanked by *TerA* and *TerB/C*. **(B)** Blue-white assays for *recD*$^+$ and Δ*recD* derivatives each carrying the indicated number of I-SceI sites (positions denoted in parentheses); all strains (i) were Δ*dnaA* with *dnaA*$^+$ shelter plasmid pHYD2388, (ii) carried the gene encoding I-SceI enzyme under control of $P_{ara}$, and (iii) were plated on Ara-supplemented medium. Representative images are shown, and the numbers beneath each of the panels indicate the percentage of white colonies to the total, that is, viable even in absence of *dnaA*$^+$ shelter plasmid (minimum of 500 colonies counted). Examples of white colonies are marked by yellow arrows. Strains employed for the different sub-panels were pHYD2388 derivatives of (all strain numbers are prefixed with GJ): i, 16079; ii, 15853; iii, 15857; iv, 15861; v, 15864; vi, 16080; vii, 15888; viii, 15892; ix, 15896; and x, 15899. **(C, D)** Dilution-spotting assays on plates supplemented with 0.2% glucose (Glu) or Ara, of blue or white colonies sourced from plates of panel B; for the top two rows on the plates of panel D, the white colonies were sourced from plates shown, respectively, in Fig. 8 iii and Fig. 4 iii.

**Figure 2**

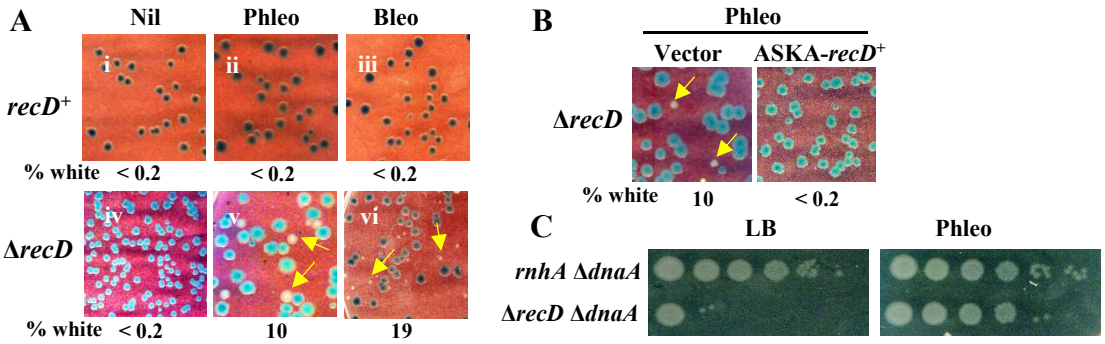


**Figure 2:** Rescue of Δ*dnaA* lethality by Δ*recD* in presence of sublethal Phleo or Bleo. **(A, B)** Blue-white assay results with pHYD2388 derivatives of GJ18607 (*recD*$^+$) or GJ15935 (Δ*recD*) are depicted as described in legend to Fig. 1B, on plates without or with Phleo or Bleo supplementation. In panel B, the Δ*recD* strain also carried the ASKA plasmid vector (pCA24N) or the latter's *recD*$^+$ derivative. **(C)** Dilution-spotting assays on medium without or with Phleo supplementation, of white colonies from plates shown in Fig. 8 iii (for top row) and Fig. 2A v (for bottom row).

**Figure 3**

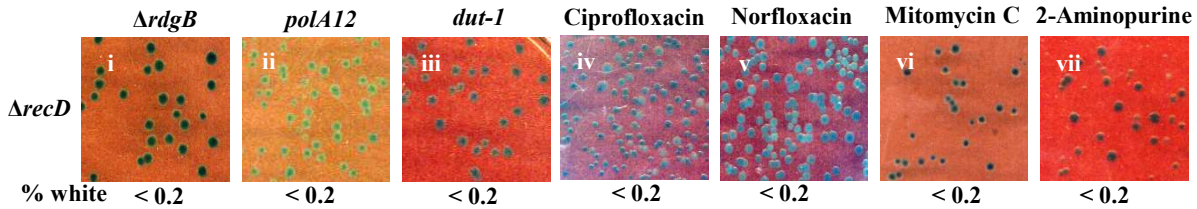


**Figure 3:** Δ*dnaA* lethality is not rescued in Δ*recD* strain by perturbations generating one-ended DSBs. Blue-white assay results are depicted, as described in legend to Fig. 1B, for Δ*recD* derivatives subjected to one-ended DSBs through either additional mutations (panels i-iii) or exposure to genotoxic agents (panels iv-vii), as indicated. Concentrations used were (µg/ml): norfloxacin, 0.02; ciprofloxacin, 0.005; mitomycin C, 1; and 2-aminopurine, 20. Strains used for the different panels were pHYD2388 derivatives of the following (all strain numbers are prefixed with GJ): i, 15939; ii, 15940; iii, 16082; and iv-vii, 15936.

**Figure 4**

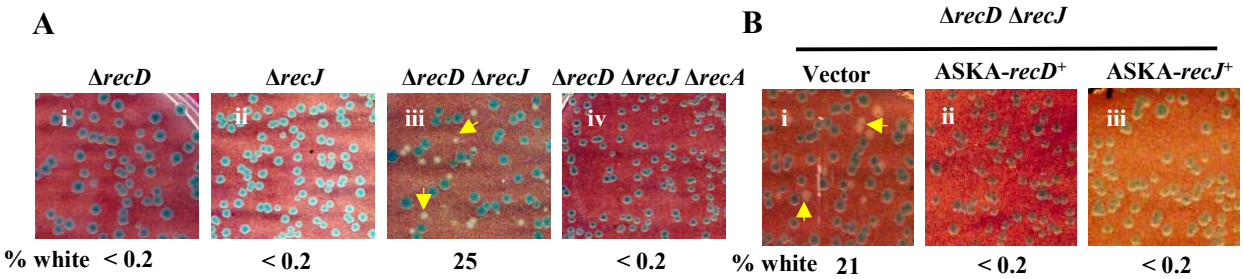


**Figure 4:** Rescue of Δ*dnaA* lethality by Δ*recD* Δ*recJ*. **(A, B)** Blue-white assay results are depicted, as described in legend to Fig. 1B, for derivatives whose relevant genotypes are given on top (all were Δ*dnaA/dnaA*$^+$). Strains used for different sub-panels of panel A were pHYD2388 derivatives of the following (all strain numbers are prefixed with GJ): i, 15936; ii, 16083; iii, 15949; and iv, 16084. In panel B, the pHYD2388 derivative of Δ*recD* Δ*recJ* strain GJ15949 also carried the ASKA plasmid vector (pCA24N) or the latter's *recD*$^+$ or *recJ*$^+$ derivative.

**Figure 5**

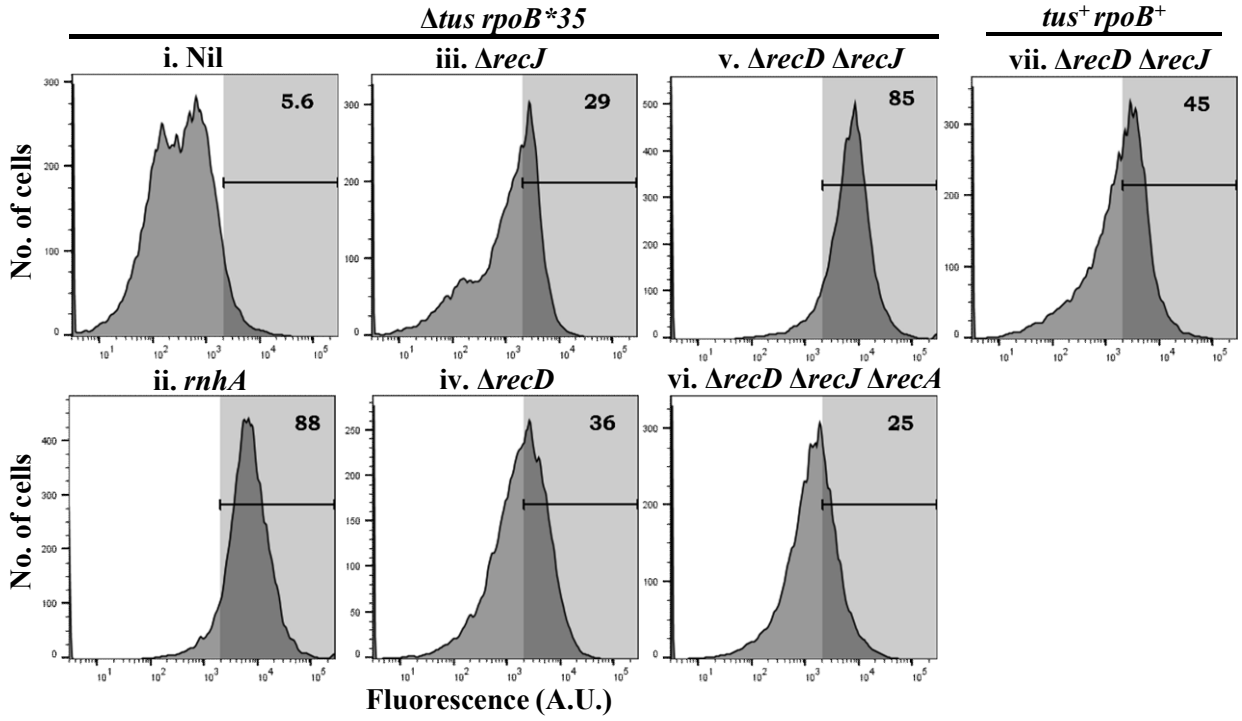


**Figure 5**: Demonstration by flow cytometry of cSDR in Δ*recD* Δ*recJ* mutants. DNA synthesis was measured as described (29, 45), for different strains (genotype given on top of each panel) after addition of spectinomycin to the cultures. In each panel, the percentage of cells in which the fluorescence value exceeded the threshold (denoted by vertical line) set at 2 X $10^3$ arbitrary units (A.U.) is given at top right. Strains used for the different panels were (all strain numbers are prefixed with GJ): i, 18609; ii, 15981; iii, 15985; iv, 15984; v, 15986; vi, 15987; and vii, 15979.

**Figure 6**

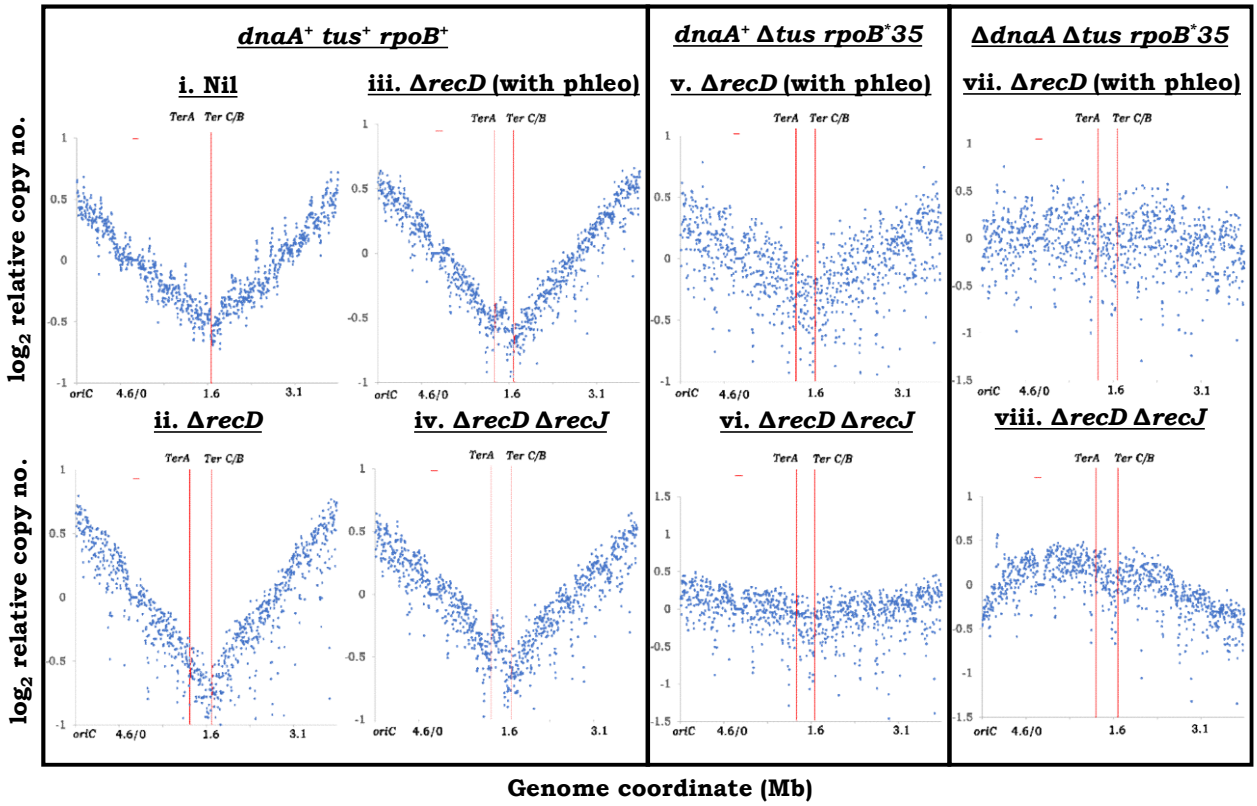


**Figure 6**: Chromosomal DNA copy number analysis by WGS. Distinguishing strain genotypes and Phleo supplementation were as indicated on top of the panels. DNA copy numbers are plotted (after normalization) as moving averages across the genome. For these graphical representations, the circular 4642-kb long chromosome is shown linearized at *oriC*, with genome coordinates on the abscissa corresponding to the MG1655 reference sequence (wherein *oriC* is at 3926 kb); the positions of *TerA* and *TerC/B* are marked. Strains used for the different panels were (all strain numbers are prefixed with GJ): i, 18601, ii-iii, 15988; iv, 15991; v, 15984; vi, 15986; vii, 15936; and viii, 15949.

**Figure 7**

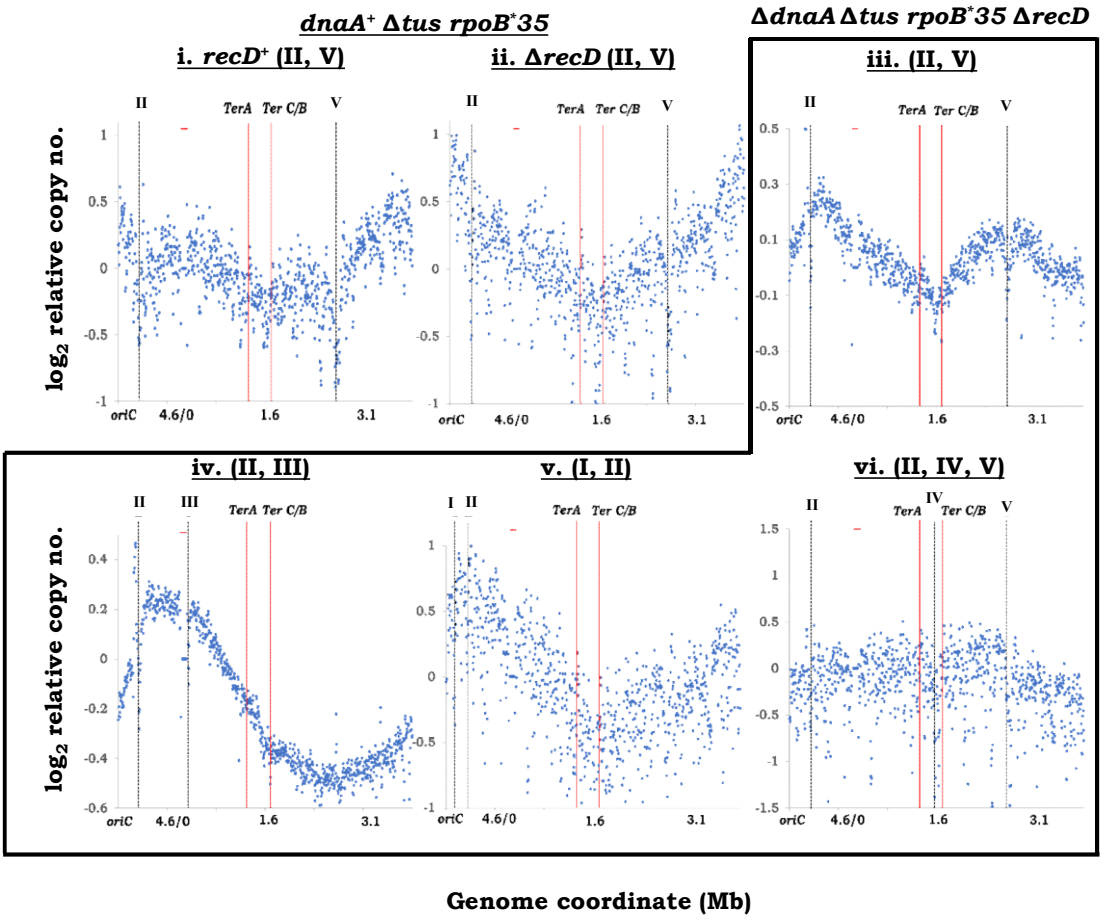


**Figure 7**: Chromosomal copy number distributions, as determined by WGS, in Δ*dnaA* Δ*recD* strains rendered viable by I-SceI cleavages. Distinguishing strain genotypes are indicated on top of the panels, and Roman numerals within parentheses denote the distinct I-SceI sites as shown in Fig. 1A; all strains also carried the construct for Ara-inducible expression of I-SceI enzyme, and were cultured in continuous presence of Ara for these experiments. Representations of WGS analysis data and notations used are as in the legend to Fig. 6; positions of I-SceI sites are also marked in each of the panels. Strains used for the different panels were (all strain numbers are prefixed with GJ): i, 15857/pHYD2388; ii, 15892/pHYD2388; iii, 15892; iv, 15889; v, 15890; and vi, 15896.

**Figure 8**

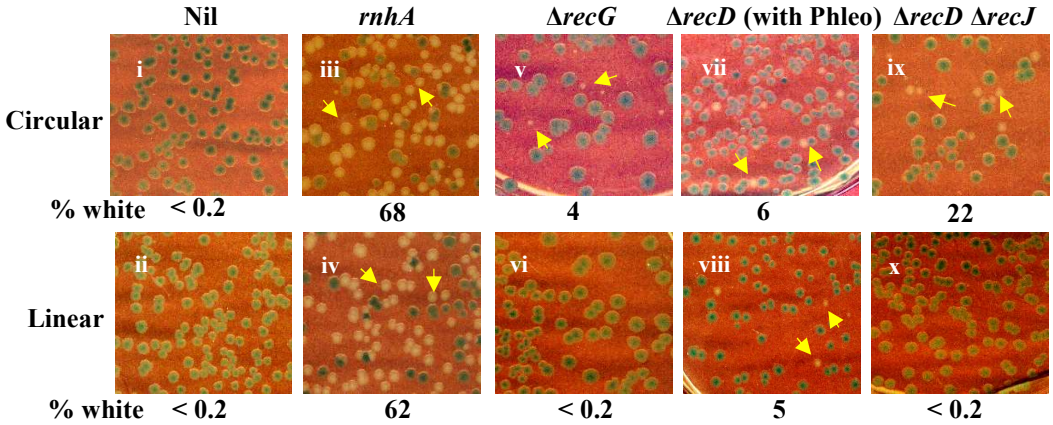


**Figure 8**: Effect of chromosome linearization on rescue of Δ*dnaA* lethality by different perturbations. Blue-white assay results are depicted, as described in legend to Fig. 1B, for isogenic pairs of circular- and linear-chromosome strains (upper and lower rows, respectively) with relevant perturbations as indicated on top. The proportion of white colonies to total was consistently elevated in *rnhA* mutants compared to that in other strains (see also Fig. 9), the reasons for which remain to be determined. Strains used for the different panels were pHYD2388 derivatives of the following (all strain numbers are prefixed with GJ): i, 18607; ii, 15993; iii, 16081; iv, 15995; v, 16464; vi, 15999; vii, 15936; viii, 16001; ix, 15949; and x, 16003.

**Figure 9**

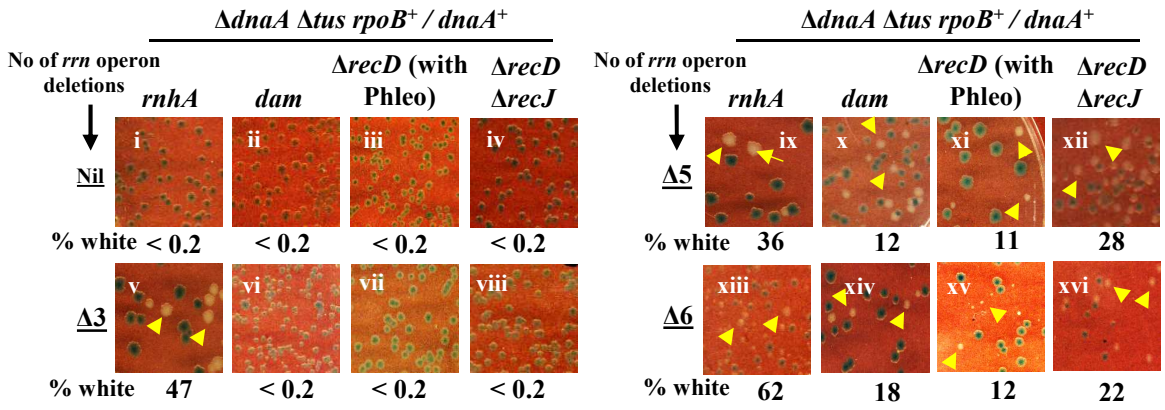


**Figure 9**: Dispensability of *rpoB*35* for cSDR-mediated Δ*dnaA* viability in Δ*rrn* strains. Blue-white assay results are depicted, as described in legend to Fig. 1B, for strains whose genotypes are indicated on top of the panels, and which bear the indicated number of *rrn* operon deletions as indicated on left for each row. Strains used for the different panels were pHYD2388 derivatives of the following (in order from left to right for each row; all strain numbers are prefixed with GJ): Nil, 16074 to 16077; Δ3, 16033 to 16036; Δ5, 16053 to 16056; and Δ6, 16063 to 16066.

**Figure 10**

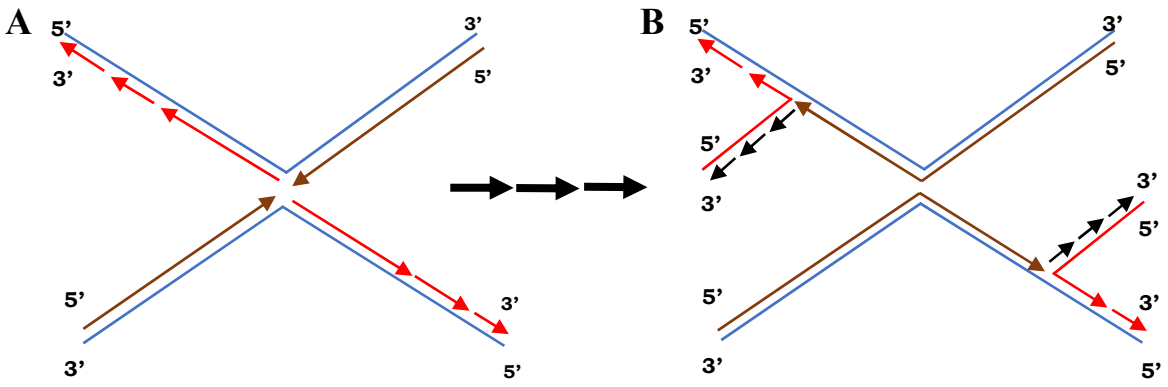


**Figure 10**: Model to explain cSDR in strains lacking RecD and RecJ. (**A**) Schematic depiction of disposition of DNA strands at a site of converging replication forks, as would occur (i) in the chromosomal terminus region before replication termination, and (ii) during ends-in replication for two-ended DSB repair. (**B**) Progression of components of one replisome past those of the other is postulated to result, ultimately, in generation of a 5'-flap (red) on the opposite lagging strand and assembly of replication restart machinery to initiate a type of rolling-circle (σ-mode) replication. Please see text for details.